Extremophiles (2020) 24:71–80
https://doi.org/10.1007/s00792-019-01131-6

SPECIAL FEATURE: ORIGINAL PAPER

12th International Congress on Extremophiles

Diverse respiratory capacity among *Thermus* strains from US Great Basin hot springs

En-Min Zhou[1,2,3] · Arinola L. Adegboruwa[3] · Chrisabelle C. Mefferd[3] · Shrikant S. Bhute[3] · Senthil K. Murugapiran[3] · Jeremy A. Dodsworth[4] · Scott C. Thomas[3] · Amanda J. Bengtson[3,5] · Lan Liu[2] · Wen-Dong Xian[2] · Wen-Jun Li[2] · Brian P. Hedlund[3,6]

Received: 31 May 2019 / Accepted: 14 August 2019 / Published online: 18 September 2019

Abstract

Thermus species are thermophilic heterotrophs, with most capable of using a variety of organic and inorganic electron donors for respiration. Here, a combined cultivation-independent and -dependent approach was used to explore the diversity of *Thermus* in Great Boiling Spring (GBS) and Little Hot Creek (LHC) in the US Great Basin. A cultivation-independent 16S rRNA gene survey of ten LHC sites showed that *Thermus* made up 0–3.5% of sequences and were predominately *Thermus thermophilus*. 189 *Thermus* isolates from GBS and LHC were affiliated with *T. aquaticus* (73.0%), *T. oshimai* (25.4%), *T. sediminis* (1.1%), and *T. thermophilus* (0.5%), with *T. aquaticus* and *T. oshimai* forming biogeographic clusters. 22 strains were selected for characterization, including chemolithotrophic oxidation of thiosulfate and arsenite, and reduction of ferric iron, polysulfide, and nitrate, revealing phenotypic diversity and broad respiratory capability within each species. PCR demonstrated the wide distribution of aerobic arsenite oxidase genes. A GBS sediment metaproteome contained sulfite oxidase and Fe^{3+} ABC transporter permease peptides, suggesting sulfur and iron transformations in situ. This study expands our knowledge of the physiological diversity of *Thermus*, suggesting widespread chemolithotrophic and anaerobic respiration phenotypes, and providing a foundation for better understanding the ecology of this genus in thermal ecosystems.

Keywords *Thermus* · Great Basin · Great Boiling Spring · Little Hot Creek · Respiratory capacity

Abbreviations

LHC Little Hot Creek
GBS Great Boiling Spring

Communicated by M. Moracci.

This manuscript is part of a special issue of Extremophiles journal for the 12th International Congress of Extremophiles (Extremophiles 2018) that was held on 16–20 September 2018 in Ischia, Naples, Italy.

Electronic supplementary material The online version of this article (https://doi.org/10.1007/s00792-019-01131-6) contains supplementary material, which is available to authorized users.

✉ Wen-Jun Li
liwenjun3@mail.sysu.edu.cn

✉ Brian P. Hedlund
brian.hedlund@unlv.edu

[1] School of Resource Environment and Earth Science, Yunnan University, Kunming 650091, People's Republic of China

[2] State Key Laboratory of Biocontrol and Guangdong Provincial Key Laboratory of Plant Resources, School of Life Sciences, Sun Yat-Sen University, Guangzhou 510275, People's Republic of China

[3] School of Life Sciences, University of Nevada Las Vegas, Las Vegas, NV, USA

[4] Department of Biology, California State University, San Bernardino, CA, USA

[5] SWCA Environmental Consultants, Reno, NV, USA

[6] Nevada Institute of Personalized Medicine, University of Nevada Las Vegas, Las Vegas, NV, USA

Introduction

After the first isolates were obtained from geothermal areas in Yellowstone National Park, USA, additional members of the genus *Thermus* have been found all over the world (Albuquerque et al. 2018; Brock and Freeze 1969). They inhabit both natural and artificial thermal environments, including terrestrial and marine hydrothermal areas, hot water taps, self-heating compost piles, and deep mines, with temperature ranging from 55 to > 80 °C, and pH from 5.0 to 10.5 (Albuquerque et al. 2018). *Thermus* strains are widely studied as model thermophilic bacteria because most of them can grow to high cell densities under laboratory conditions and some possess a highly efficient natural competence system that enables genetic manipulation (Averhoff 2009). *Thermus* species are also well known as sources of thermostable enzymes (Pantazaki et al. 2002; Vieille and Zeikus 2001) and have been useful for elucidation of molecular mechanisms conferring thermophily (Sazanov and Hinchliffe 2006; Yusupov et al. 2001).

Although major advances have been made with *Thermus* species, current knowledge about their physiology, geographic distribution, and ecological roles is not complete. *Thermus* species are known to utilize a variety of organic substrates for growth and are obligately respiratory. A few strains are obligately aerobic, notably *T. aquaticus, T. sediminis,* and *T. composti*, but most are capable of growth under anaerobic conditions using NO_3^-, Fe^{3+}, or S^0 as terminal electron acceptors (Balkwill et al. 2004; Kieft et al. 1999). Some *Thermus* species have also been found to grow by oxidation of As^{3+} (Gihring et al. 2001; Zhou et al. 2018), a metalloid known to be toxic and a possible factor in the development of arsenicosis. However, those results were observed with a very limited diversity of *Thermus* strains.

This study builds on previous studies on the biology of *Thermus* in geothermal springs in the Great Basin, including studies that possibly link incomplete denitrifiers belonging to *T. thermophilus* and *T. oshimai* to high nitrous oxide flux from high-temperature sites within Great Boiling Spring (GBS), NV (Hedlund et al. 2011; Murugapiran et al. 2013) and the description of a novel species, *T. sediminis*, from Little Hot Creek (LHC), CA (Zhou et al. 2018). The objectives of this study were to assess the diversity of *Thermus* group from these two geothermal systems using both cultivation-dependent and -independent approaches. In addition, representative strains were characterized with regard to electron donors for chemolithotrophy and terminal electron acceptors for anaerobic respiration.

Materials and methods

Sample collection and cultivation-independent census of bacteria and archaea

Samples were obtained from GBS (GPS location N40°39.686′, W119°21.980′), NV, and Little Hot Creek [LHC1, GPS location N37°41.436′ W118°50.664′ and LHC3, GPS location N37°41.456′ W118°50.639′ (Vick et al. 2010)] in the Long Valley Caldera, CA, USA. Temperature and pH were measured at the precise sampling sites with a field-calibrated pH probe with temperature correction (LaMotte five Series, Chestertown, MD, USA), and then water, surface sediments, and mat samples were collected into 15 mL polypropylene tubes for later laboratory cultivation, described below. Following homogenization, LHC sediments in the 15 mL tubes were subsampled and frozen on dry ice for cultivation-independent surveys. The location and basic physicochemical characteristics of each sampling site are summarized in Table 1 and Fig. 1.

DNA was extracted from sediment samples using the FastDNA™ SPIN Kit for Soil (MP Biomedicals, Santa Ana, CA). The concentration and purity of extracted DNA were checked using the NanoDrop ND-2000 spectrophotometer (Thermo Fisher Scientific, Wilmington, USA). The V4 region of the 16S rRNA was amplified with the updated bacterial- and archaeal-specific 515F/806R primer set with a 12 bp barcode using the following PCR conditions: the reaction mix (50 µL) contained 25 µL 2 × Premix Taq (Takara Biotechnology, Dalian Co. Ltd., China), 0.1 µM of each primer, 10 ng of template, and 20 µL of Nuclease-free water. PCR thermocycling included 5 min at 94 °C for initialization; 30 cycles of 94 °C for 30 s, 52 °C for 30 s, and 72 °C for 30 s; followed by 10 min final elongation at 72 °C. The PCR products were detected by 1% agarose gel electrophoresis and purified. Sequencing libraries were generated using NEBNext® Ultra™ DNA Library Prep Kit for Illumina® (New England Biolabs, Ipswich, MA, USA) following manufacturer's recommendations, and index codes were added. Finally, the library was subjected to the Illumina HiSeq 2500 platform (Guangdong Magigene Biotechnology Co., Ltd. China). Paired-end reads were quality filtered, aligned, and analyzed using the 2018.4.0 version of Qiime2 (Caporaso et al. 2010; https://qiime2.org/). Quality filtering of reads and removal of chimera sequences was performed using the q2-dada2 (Callahan et al. 2016) plugin. Reads were truncated at the first base with PHRED score < 30. Following clustering, sequence variants were aligned using mafft (Katoh and Standley 2013) through the q2-alignment plugin using default settings. Sequence variants were then taxonomically classified using the Silva nr. 99 reference

Table 1 Basic information on hot spring sampling sites and isolated *Thermus* species

Hot springs	Sampling sites	Temperature (°C)	pH	Description of samples	Number of *Thermus* isolations
GBS	GBS-A	76.8	7.1	Fine gray sediment	*T. aquaticus* (18); *T. oshimai* (1)
	GBS-B	70.2	7.1	Gray sediment, brown mat	*T. aquaticus* (12); *T. oshimai* (6); *T. thermophilus* (1)
	GBS-C	64.7	7.1	Brown mat, gray sediment	*T. aquaticus* (16)
	GBS-D	59.9	7.1	Brown mat and sediment	*T. aquaticus* (10)
	GBS-E	55.6	7.1	Brown mat and sediment	*None*
	GBS-F	50.9	7.1	Dark brown mat and sediment	*T. aquaticus* (3)
	GBS-G	46.2	7.1	Green/brown mat and sediment	*None*
LHC1	LHC1-D	80.0	6.8	Black/brown sediment	*T. aquaticus* (5); *T. sediminis* (1)
	LHC1-F	75.0	7.3	Fine brown sediment	*T. aquaticus* (8); *T. oshimai* (12)
	LHC1-G	71.7	7.7	Gray sediment, green mat	*T. aquaticus* (23); *T. oshimai* (13)
	LHC1-H	65.0	7.9	Gray sediment, green/brown mat	*T. aquaticus* (10); *T. oshimai* (2); *T. sediminis* (1)
	LHC1-I	60.0	8.2	Green/brown flakey mat and sediment	*T. aquaticus* (5); *T. oshimai* (7)
	LHC1-J	55.6	8.4	Brown mat and sediment	*None*
	LHC1-K	50.0	8.6	Green/brown flakey mat and sediment	*None*
	LHC1-L	44.9	8.7	Green mat and sediment	*None*
LHC3	LHC3-2	76.2	6.8	Black sediment	*T. aquaticus* (20); *T. oshimai* (5)
	LHC3-3	73.7	6.9	Brown sediment	*T. aquaticus* (8); *T. oshimai* (2)

GBS Great Boiling Spring, *LHC1* Little Hot Creek Spring 1, *LHC3* Little Hot Creek Spring

database with the classify-sklearn function of the q2-feature-classifier plugin. After sequence processing, taxonomy, abundance, and metadata tables were imported into R and turned into a single operable object using phyloseq version 1.22.3 (McMurdie and Holmes 2013). Alpha-diversity metrics were generated using phyloseq and ggplot2 version 2.2.1 was used to visualize the taxonomy data (Wickham 2009). All DNA sequence data described in this paper are available under NCBI BioProject and NCBI BioSamples SAMN12113068–SAMN12113077. Files containing the original unfiltered 16S rRNA gene Illumina amplicons are available from the NCBI Sequence Read Archive under PRJNA550208.

Isolation of *Thermus* strains

Samples for cultivation were transported to laboratory in the dark without temperature control. Within two days of collection, 1 g of sediment or microbial mat from each sampling site was homogenized using a mortar and pestle, suspended in 9 mL of sterile water, vortex for 10 min, serially diluted, and plated onto R2A, T5 (Yu et al. 2013), *Thermus* medium (Castenholz, 1969), and *Thermus* 162 plates (Degryse et al. 1978). All plates were incubated aerobically within Tupperware containers at temperatures similar to the sampling sites. *Thermus*-like isolates were randomly selected based on colony morphology after 5 days of incubation and restreaked at least three times on *Thermus* medium; incubation temperatures were modified to accommodate strains that grew better at lower temperatures. Isolates were then routinely cultured on *Thermus* medium at 65 °C and stored at − 80 °C as glycerol suspensions (20%, v/v).

Isolate 16S rRNA and *aioA* gene PCR, sequencing, and phylogenetic analysis

DNA for PCR was prepared by the colony lysis procedure described by Johnson et al. (2001). The nearly full-length 16S rRNA gene was amplified from all isolations by PCR with the primers 9bF (5′-GRGTTTGATCCTGGCTCAG) and 1512uR (5′-ACGGGCGGTGTGTRCAA), as generally described by Eder et al. 2001. PCR reagents and cycling conditions were performed as described previously (Hedlund et al. 2011). PCR for the *aioA* gene from representative strains was carried out using the degenerate primers *aioA*-95f (5′-TGYCABTWCTGCAIYGYIGG-3′) and *aioA*-599r (5′-TCDGARTTGTASGCIGGICKRTT-3′) as described by Hamamura et al. (2009). PCR products for both 16S rRNA and *aioA* genes were sequenced with the forward PCR primer using the Sanger method at Functional Biosciences, Madison, WI. Reads were trimmed to remove bases with quality scores less than 20. The 16S rRNA gene sequences were aligned using the mothur-provided SILVA alignment in mothur v.1.39.5 (Schloss et al. 2009). The mothur-provided SILVA-compatible 1349-position Lane mask was applied to manually correct the alignment. Phylogenetic analyses were performed using neighbor-joining (Saitou and Nei 1987) and maximum-likelihood (Felsenstein 1981) methods by using

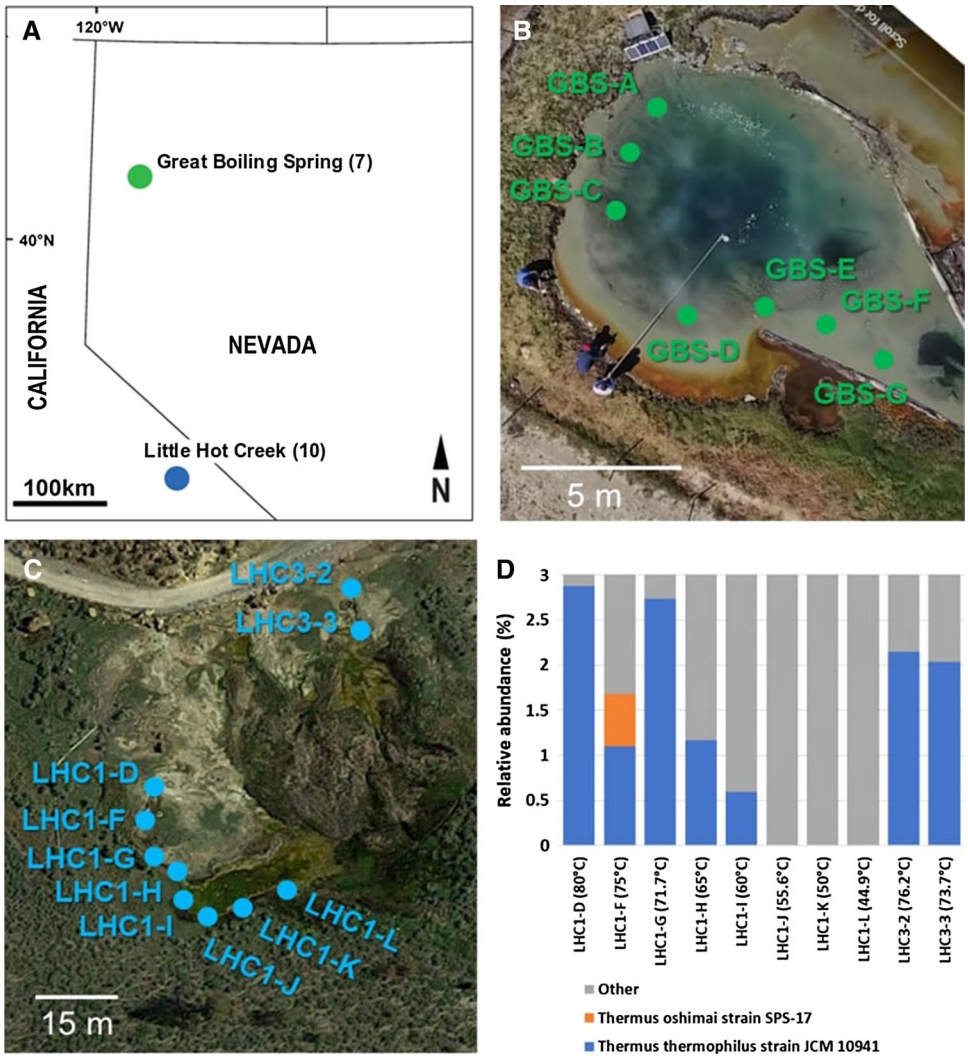

Fig. 1 Sampling locations and abundance of *Thermus*. **a** Location of sampling sites in the western US; **b** drone photo of GBS with sampling locations indicated (used with permission from https://www.youtube.com/watch?v=0FUX9VJSwcE); **c** satellite photo of LHC with sampling sites identified (google maps); and **d** relative abundance of *Thermus* 16S rRNA gene sequences in Illumina tag analysis at LHC

software package MEGA version 7.0 (Kumar et al. 2016). The topology of the phylogenetic trees was evaluated by the bootstrap resampling method of Felsenstein with 1000 resamplings (Felsenstein 1985).

A section of *aioA* corresponding to the *T. thermophilus* HB8 amino acid positions 581–753 was aligned with related *aioA* and deduced AioA sequences using default parameters of ClustalW within BioEdit (Hall 2011). All alignments were checked manually and gaps at the 5′ and 3′ ends of the alignment were omitted from the analysis. Phylogenetic analyses were performed using the MEGA version 7.0 (Kumar et al. 2016) with neighbor-joining (Saitou and Nei 1987) and maximum-likelihood (Felsenstein 1981) algorithms. The topology of all phylogenetic trees was evaluated by the bootstrap resamplings method with 1000 resamplings (Felsenstein 1985). NCBI accession numbers for near-complete 16S rRNA genes and *aioA* genes are MN252488–MN252509 and MN256131–MN256144, respectively.

Phenotypic characterization of respiratory capacity

Based on the phylogenetic position and isolation source (Table 2), a subset of 22 strains was selected for phenotypic characterization of respiratory capacity. Nitrate reduction ability was assayed based on strains' ability to grow in anaerobic *Thermus* medium containing 9 mM nitrate at 65 °C, as described by Hedlund et al. (2011). Nitrite and residual nitrate were measured colorimetrically to confirm that nitrate was reduced. Polysulfide reduction ability was detected by observing a zone of clearing in TYG medium (5 g tryptone, 3 g yeast extract, and 1 g glucose per liter) containing 30 mM S^0, 30 mM lactate, and 20 g of agar per liter according to Moser and Nealson et al. (1996), and Kieft et al. (1999). A defined basal medium with 10 mM Fe(III)-NTA or Fe(III)-citrate used by Kieft et al. (1999) was selected to assess the iron reduction of *Thermus* strains under anaerobic growth condition. Thiosulfate oxidation ability was detected by measuring an increase in sulfate according to the method

Table 2 Information on respiratory capacity of 22 representative *Thermus* strains and physiological traits

Strain	Closest match	Identity (%)	Isolation source	Thiosulfate oxidation	Arsenite oxidation	Nitrate reduction	Polysulfide reduction	Ferric NTA reduction	Ferric citrate reduction
G104	*T. aquaticus* YT-1 T	98.66	GBS-A	P	N*	N	P	N	N
G117	*T. oshimai* DSM 12092 T	99.77	GBS-A	P	N	P	P	P	P
G125	*T. aquaticus* YT-1 T	98.96	GBS-A	P	P*	N	P	P	P
G145	*T. aquaticus* YT-1 T	98.58	GBS-B	N	N	N	P	N	N
G146	*T. oshimai* DSM 12092 T	99.77	GBS-B	N	N	N	P	N	N
G159-2	*T. thermophilus* HB8T	99.85	GBS-B	P	N	P	P	P	N
G159-3	*T. aquaticus* YT-1 T	98.28	GBS-B	P	P*	P	P	N	N
G163-1	*T. oshimai* DSM 12092 T	99.78	GBS-B	P	N	P	P	P	P
G164	*T. oshimai* DSM 12092 T	99.78	GBS-B	P	N	P	P	P	P
L198	*T. islandicus* DSM 21543 T	96.88	LHC1-H	P	N	N	N	N	N
L423	*T. arciformis* TH92T	96.74	LHC1-D	P	N	N	N	N	N
L228	*T. aquaticus* YT-1 T	98.1	LHC1-G	N	N*	N	N	N	N
L229	*T. aquaticus* YT-1 T	98.18	LHC1-G	P	N*	N	P	P	P
L234	*T. oshimai* DSM 12092 T	99.64	LHC1-G	P	P*	P	P	P	P
L235	*T. oshimai* DSM 12092 T	99.71	LHC1-G	P	P*	P	P	P	P
L241	*T. oshimai* DSM 12092 T	99.78	LHC1-G	P	P*	P	P	P	P
L275	*T. aquaticus* YT-1 T	97.98	LHC3-3	P	N*	P	P	P	P
L297	*T. aquaticus* YT-1 T	98.04	LHC3-3	N	N*	N	N	N	N
L313	*T. oshimai* DSM 12092 T	99.85	LHC3-2	N	N*	P	P	P	P
L354	*T. aquaticus* YT-1 T	99.78	LHC3-2	N	N*	N	N	N	N
L397	*T. oshimai* DSM 12092 T	98.15	LHC1-F	P	P*	P	P	P	P
PS-3	*T. aquaticus* YT-1 T	97.9	LHC1-I	P	N*	N	P	P	P

P positive, *N* negative, *NTA* nitrile triacetic acid

*Strains with a putative *aioA* gene

of Skirnisdottir et al. (2001). Arsenite oxidation ability was detected by measuring removal of arsenite according to the method of Gihring et al. (2001).

Metaproteomics analysis from GBS sediments

Total protein was extracted from native GBS sediments collected from site GBS-A (Fig. 1b) in 1 mL SDS cell lysis buffer and bead beating in Lysis Matrix E (MP Biomedicals), followed by TCA precipitation, resuspension, iodoacetamide treatment, and tryptic digestion (Pan and Banfield 2014), yielding 14 µg of protein from 1 mL GBS sediment slurry (~0.3 g dry mass). Protein was digested with trypsin and analyzed using liquid chromatography with online electrospray tandem mass spectrometry (LC–MS/MS) at the UC Davis Proteomics Core. Tandem mass spectrometry data files were converted to mzXML format. *Thermus oshimai* JL-2 and *Thermus thermophilus* JL-18 protein fasta files from NCBI RefSeq were used to search against GBS sediment metaproteome tandem mass spectra using Crux pipeline (Park et al. 2008) with the default options except the following: –compute-sp T-exact-*p*-value T-score-function both—bullseye F. Only those peptide spectrum matches (PSM) that satisfied the filter criteria of percolator posterior error probability (PEP) < 0.01 were considered. A similar search repeated using the same parameters with *E. coli* K12 protein file as a negative control did not yield any hits at the same filtering cutoff of PEP < 0.01. In all searches, a list of common protein contaminants obtained from the Global Proteome Machine (ftp://ftp.thegpm.org/fasta/cRAP) was used to identify and remove hits to contaminant peptide hits to trypsin, keratin, and others.

Results and discussion

Distribution of *Thermus* species along temperature gradients

The V4 region of the 16S rRNA gene was amplified and sequenced from community DNA from ten samples in LHC1 and LHC3 to assess the abundance, location, and identity of *Thermus* species in that system. *Thermus* sequences were present in the source pools of LHC1 and LHC3 at ~ 3.5%

and ~ 2.5%, respectively, with a general trend of decreasing relative abundance in the outflow of LHC1 (Fig. 1); *Thermus* was not detected in samples ≤ 55.6 °C. Nearly all sequences (>99%) were assigned to *Thermus thermophilus*, which is in accordance with these strains being inhabitants of the high-temperature sources. The remaining sequences could be identified to the genus, but not a species.

Isolation, identification, and biogeography of *Thermus* isolates

17 different locations were sampled from GBS and LHC, including the same samples used for the cultivation-independent census, with a total of 189 strains isolated. There was perfect concordance between LHC samples in which *Thermus* strains were detected in the cultivation-independent census and were successfully isolated; however, the identity of the isolates was different from the cultivation-independent survey. Analysis of near full-length 16S rRNA gene sequences showed that all strains belonged to the genus *Thermus*, with most being closely related to *T. aquaticus* (73.0%), followed by *T. oshimai* (25.4%), *T. sediminis* (1.1%), and *T. thermophilus* (0.5%) (Table 1; Fig. 1; Figure S1). Strains closely related to *T. aquaticus* and *T. oshimai* formed two clusters that were exclusive to either geothermal system. Two isolates from LHC were most closely related to *T. composti* and *T. islandicus* and were recently described as a new species, *T. sediminis* (Zhou et al. 2018). Finally, a single strain closely related to the type strain of *T. thermophilus* was isolated from GBS.

The isolates described here correspond closely with 16S rRNA sequences from previous cultivation-independent surveys of GBS (Costa et al. 2009) and LHC (Vick et al. 2010), using near-complete 16S rRNA gene sequences and *Thermus* isolates described previously from GBS (Hedlund et al. 2011) (Fig. 2). The previous cultivation-independent census in several springs in the GBS geothermal field recovered only two phylotypes, which corresponded to the phylogenetic clusters related to *T. aquaticus* and *T. thermophilus* described in this work. These two lineages, along with a few isolates of *T. oshimai* were later isolated from GBS using several different isolation strategies (Hedlund et al. 2011). The previous cultivation-independent study of the four major sources at LHC uncovered only a single *Thermus* phylotype that belonged to the *T. aquaticus* cluster described here. Congruence between this work and the previous cultivation-independent and -dependent studies at these springs, more than five years later, suggests the isolates described in this study represent abundant and stable *Thermus* populations in these springs. However, *T. oshimai* and *T. sediminis* were not detected previously in either spring in 16S rRNA gene surveys, demonstrating the sensitivity of the *Thermus*-focused cultivation approach used here. Although the *Thermus* species retrieved here from GBS corresponded perfectly with the previous cultivation study at GBS, the relative abundance of the three *Thermus* species was different. In the previous study, most isolates belonged to *T. thermophilus*, possibly reflecting the focus of that study on high-temperature sites and incubations (80 °C) and on anaerobic enrichment and isolation procedures.

The geographical clustering observed here for *Thermus* was similar to that observed for other thermophiles, including *Sulfolobus* (Whitaker et al. 2003) and *Korarchaeota* (Miller et al. 2012). The former showed biogeographic clustering of *Sulfolobus* isolates in the scale of kilometers to continents. The latter study used PCR with *Korarchaeota*-specific primers and showed that the dominant *Korarchaeota* in Great Basin and Yellowstone National Park, close relatives of "*Candidatus* Korarchaeum kryptofilum", form distinct biogeographic clusters, yet the phylotypes in GBS and LHC were indistinguishable by 16S rRNA gene sequence. This general pattern suggests that many thermophiles do not disperse or share genes horizontally across large distances and are undergoing allopatric speciation.

Chemolithotrophy and distribution and phylogeny of arsenite oxidase genes

To narrow the phenotypic work, 22 strains were selected based on the phylogenetic position and isolation source (Table 2). The new isolates were chemoorganotrophic and grew well on complex media in the absence of inorganic electron donors under aerobic conditions. Most (20/22) were also capable of some form of chemolithotrophy, with thiosulfate oxidation being more widely detected (16/22 strains) than arsenite oxidation (6/22 strains).

Thiosulfate oxidation was demonstrated in all four groups of *Thermus* isolates and was only negative for four strains related to *T. aquaticus* and two strains related to *T. oshimai*. Thiosulfate and/or sulfur oxidation have been demonstrated in only a few species of *Thermus*, including *T. scotoductus* (Skirnisdottir et al. 2001), *T. calditerrae* (Ming et al. 2014), and *T. sediminis* (Zhou et al. 2018), although *sox* gene clusters predicted to confer thiosulfate and/or sulfur oxidation capability are widely distributed in *Thermus* genomes, including isolates from GBS (Henne et al. 2004; Mefferd et al. 2016; Murugapiran et al. 2013). Thiosulfate was shown to stimulate aerobic respiration in electron-donor limited water and sediments from GBS and nearby Sandy's Spring West (Murphy et al. 2013), and it is possible that *Thermus* may have played a role in that activity.

Arsenite oxidation was only demonstrated in two of four strains related to *T. aquaticus* both from GBS and four of five strains related to *T. oshimai* from LHC. The gene encoding the arsenite oxidase large subunit, *aioA*, was amplified by PCR from all six strains with arsenite oxidation activity,

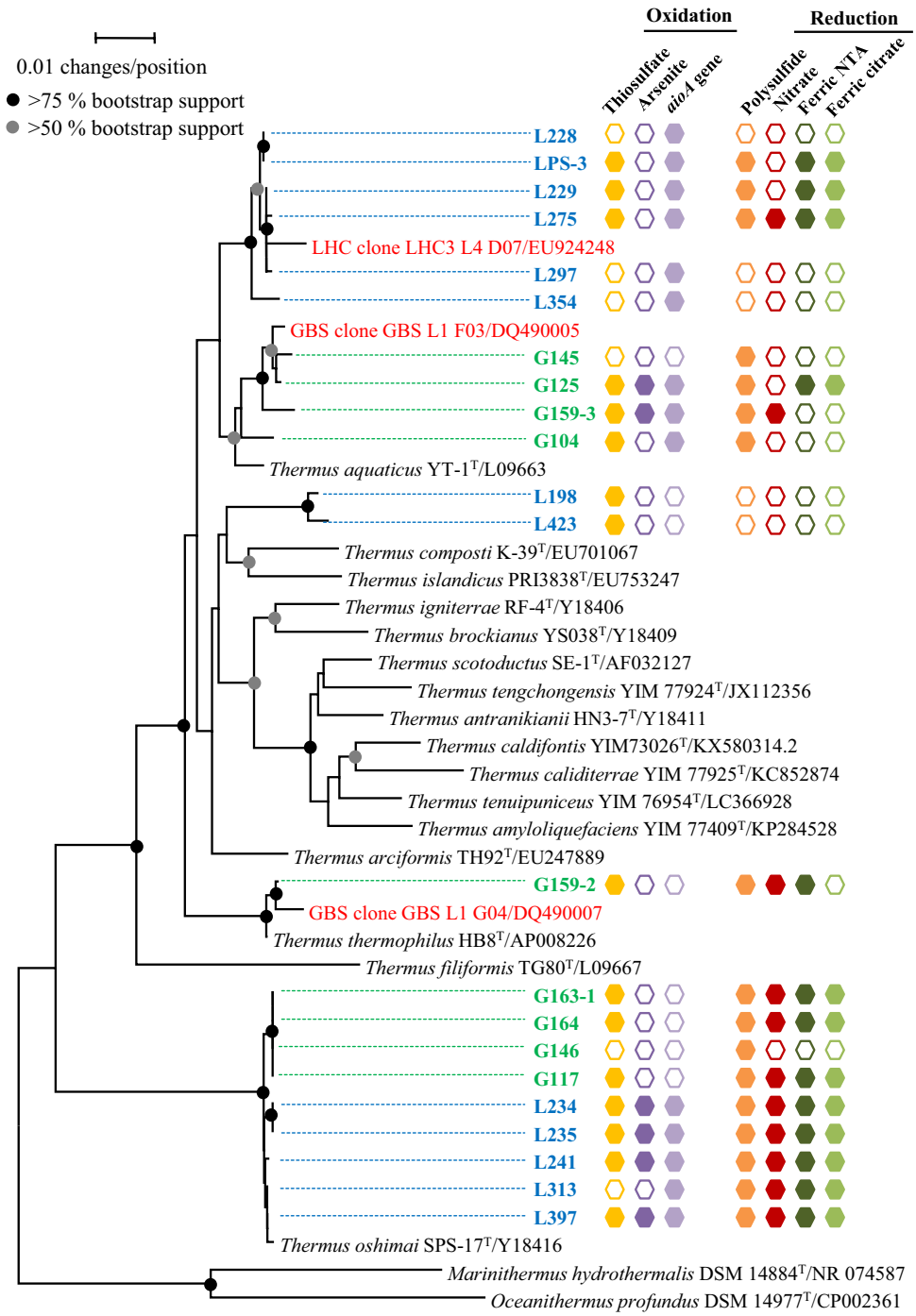

Fig. 2 Neighbor-joining phylogenetic tree of isolates from GBS (green) and LHC (blue) and reference strains based on near-complete 16S rRNA gene sequences. Respiratory capacity is summarized in hexagons, with filled hexagons representing positive results, and open hexagons representing negative results. Red text denotes near full-length 16S rRNA gene sequences from GBS (Costa et al. 2009) and LHC (Vick et al. 2010)

but also from an additional strain related to *T. oshimai* from LHC and all strains related to *T. aquaticus* except one, regardless of geographic location. The negative arsenite oxidation phenotype of the LHC *T. aquaticus* strains, despite the ubiquity of the *aioA* gene, suggests that different conditions are needed for expression of this phenotype or that their *aioA* gene does not encode a functional arsenite oxidase; however, the close phylogenetic relationship between the *aioA* genes from the GBS and LHC strains suggests the former (Figure S2). The higher prevalence of *aioA* genes in LHC strains, over GBS strains, is consistent with the higher concentration of arsenic in waters of LHC (Vick et al. 2010) over GBS (Costa et al. 2009). *T. sediminis*, although not able to oxidize arsenite, is capable of arsenate reduction under anaerobic conditions (Zhou et al. 2018). The uniform presence of *aioA* genes in *T. oshimai* strains from LHC, and their absence in related strains from GBS is consistent with the biogeographic clustering of these strains.

Anaerobic respiration phenotypes

Most strains (20/22) were capable of anaerobic respiration, with polysulfide reduction being more common (18/22 strains) than ferric iron (13/22 strains) and nitrate reduction (11/22 strains). Polysulfide reduction phenotype was only absent in two LHC strains related to *T. aquaticus* and the two *T. sediminis* strains. Polysulfide reduction has previously been demonstrated in *T. scotoductus* strains (Balkwill et al. 2004; Kieft et al. 1999), and *psrA*, *psrB*, and *psrC*, encoding the three subunits of the polysulfide reductase, are present in several *Thermus* genomes, including isolates from GBS (Murugapiran et al. 2013; Mefferd et al. 2016). Our results suggest polysulfide reduction may be very common in *Thermus*.

Almost all strains (19/22) gave positive results for iron reduction assays regardless of whether ferric iron was supplied as ferric NTA or ferric citrate. Iron reduction was observed in nearly all *T. oshimai* strains (8/9), half of the LHC *T. aquaticus* isolates (3/6), one GBS *T. aquaticus strain*, and the lone *T. thermophilus* strain; however, the *T. thermophilus* isolate only reduced ferric NTA. Iron respiration is not often studied in *Thermus*, but it has been studied in detail in *T. scotoductus* strains, which contain both soluble and membrane-associated iron reductases (Balkwill et al. 2004; Bester et al. 2010; Kieft et al. 1999; Möller and Heerden 2006). Other studies suggest iron reduction may be limited to *T. scotoductus* (Balkwill et al. 2004); however, our study suggests iron reduction is widespread in the genus.

Nitrate reduction was observed in nearly all *T. oshimai* strains (8/9), one LHC *T. aquaticus* isolate, and the *T. thermophilus* isolate. This pattern is in general agreement with nitrate reduction by other *T. oshimai* and *T. thermophilus* strains (Albuquerque et al. 2018; Hedlund et al. 2011); however, nitrate reduction has not been previously observed in *T. aquaticus* (Albuquerque et al. 2018). Previous studies have shown that *T. oshimai* and *T. thermophilus* strains from GBS and nearby springs all denitrify, with nitrous oxide as the terminal denitrification product (Hedlund et al. 2011); however, the denitrification products were not identified in the current study.

Metaproteomics

A metaproteome was generated from a sediment slurry from the GBS-A site (Fig. 1) to determine whether respiratory pathways studied here are likely to be expressed in situ. A total of 56 peptides were assigned to *T. thermophilus* and 62 to *T. oshimai*. The peptides assigned to *Thermus* included many proteins involved in major cell activities such as transcription, translation, stress response, and energy metabolism (Table S1). These proteins, and others, suggest that *Thermus* is active and growing in these sediments. Only a few peptides were assigned to proteins involved in heterotrophy (branched-chain amino acid ABC transporter components (WP_014630498.1; WP_015065207.1); general amino acid ABC transporter substrate-binding protein (WP_016329420.1); beta-glucosidase (WP_014630212.1)). Fewer were diagnostic of a particular mode of respiration. A sulfite oxidase (WP_014629340.1) assigned to *T. thermophilus* suggests sulfur-based chemolithotrophy, which is consistent with thiosulfate stimulation of oxygen consumption in GBS (Murphy et al. 2013), the presence of a 15-gene Sox pathway in *T. thermophilus* (Murugapiran et al. 2013), and the broad distribution of thiosulfate oxidation activity within *Thermus* described here, including *T. thermophilus* from GBS (Fig. 2). Additionally, an Fe^{3+} ABC transporter permease peptide was assigned to *T. oshimai*. Although this transporter could be involved in both assimilatory Fe^{3+} transport or Fe^{3+} respiration, its presence is consistent with the prevalence of iron reduction in *T. oshimai*, described here.

Conclusions

This study is one of few that integrate detailed phenotypic work with microbial pure cultures and cultivation-independent investigations of the same organisms in situ. Our results demonstrate the wide distribution and biogeographic clustering of *Thermus* strains closely related to the type strains of *T. aquaticus* and *T. oshimai* in the US Great Basin. The strains displayed remarkable diversity with respect to respiratory capacity, both with regard to electron donors for chemolithotrophy and terminal electron acceptors for anaerobic respiration. This suggests that the role of *Thermus* strains in sulfur, metal, and nitrogen biogeochemical cycles in terrestrial geothermal systems may be underestimated. Similar work has showed even broader respiratory capacity among a small number of *T. scotoductus* strains, including anaerobic respiration with Fe^{3+}, Mn^{4+}, S^0, and nitrate as terminal electron acceptors (Balkwill et al. 2004; Kieft et al. 1999). The wide distribution of arsenite oxidation activity and incidence of the *aioA* gene suggests arsenite oxidation may be underappreciated. Although the denitrification phenotypes of these strains were not studied in detail here, this and other work also support the importance of *Thermus* in denitrification in geothermal systems. The few peptide matches to proteins involved in specific respiration pathways suggest the importance of sulfur oxidations and iron reductions in situ, which is consistent with previous in situ respiration studies in GBS. We encourage further integration of cultivation- and cultivation-independent work to link activities studied in the lab to activity in situ. The importance of *Thermus* in these different biogeochemical cycles should be addressed by broader and deeper surveys into the respiratory capacity

across the genus and in different geothermal systems, combined with studies of in situ activity, possibly by metatranscriptomic and metaproteomic studies.

Acknowledgements We thank the National Forest Service (Inyo National Forest, Mammoth Lakes Office) for permission to sample Little Hot Creek and David and Sandy Jamieson for gracious support and access to Great Boiling Spring. This work was supported by the National Natural Science Foundation of China (Nos. 31600103 and 31470139), China Postdoctoral Science Foundation (2016M602569), and National Science Foundation grants (OISE-0968421 and DBI-1005223). Wen-Jun Li was also supported by Guangdong Province Higher Vocational Colleges and Schools Pearl River Scholar Funded Scheme (2014). B.P. Hedlund was also funded by a gift from Greg Fullmer through the UNLV Foundation.

Author Contributions EMZ, WJL and BPH conceived and designed the experiments; EMZ, JAD, SKM collected the samples; EMZ, ALA, CCM, SSB, AJW, LL, and WDX performed the experiments and analyzed the data; JAD, SCT, ALA, BPH, and WJL supervised the experiment. All authors assisted in writing the manuscript, discussed the results and commented on the manuscript.

Compliance with ethical standards

Conflict of interest The authors declare that the research was conducted in the absence of any commercial or financial relationships that could be construed as a potential conflict of interest.

References

Albuquerque L, Rainey FA, Da Costa MS (2018) *Thermus*. In: Whitman WB et al. (eds) Bergey's manual of systematics of archaea and bacteria. https://doi.org/10.1002/9781118960608.gbm00477.pub2

Averhoff B (2009) Shuffling genes around in hot environments: the unique DNA transporter of *Thermus thermophilus*. FEMS Microbiol Rev 33:611–626. https://doi.org/10.1111/j.1574-6976.2008.00160.x

Balkwill DL, Kieft TL, Tsukuda T, Kostandarithes HM, Onstott TC, Macnaughton S, Bownas J, Fredrickson JK (2004) Identification of iron-reducing *Thermus* strains as *Thermus scotoductus*. Extremophiles 8:37–44

Bester PA, Litthauer D, Piater LA, van Heerden E (2010) A thioredoxin reductase-like protein from the thermophile, *Thermus* scotoductus SA-01, displaying iron reductase activity. FEMS Microbiol Lett 302:182–188. https://doi.org/10.1111/j.1574-6968.2009.01852.x

Brock TD, Freeze H (1969) *Thermus aquaticus* gen. n. and sp. n., a nonsporulating extreme thermophile. J Bacteriol 98:289–297

Callahan B, McMurdie P, Rosen M, Han A, Johnson A, Holmes S (2016) DADA2: High-resolution sample inference from Illumina amplicon data. Nat Methods 13:581–583. https://doi.org/10.1038/nmeth.3869

Caporaso JG, Kuczynski J, Stombaugh J, Bittinger K, Bushman F, Costello E, Fierer N, Pena A, Goodrich J, Godron J, Huttley G, Kelley S, Knights D, Koenig J, Ley R, Lozupone C, McDonald D, Muegge B, Pirrung M, Reeder J, Sevinsky J, Turnbaugh P, Walters W, Widmann J, Yatsunenko T, Zaneveld J, Knight R (2010) QIIME allows analysis of high-throughput community sequencing data. Nat Methods 7:335–336. https://doi.org/10.1038/nmeth.f.303

Castenholz RW (1969) Thermophilic blue-green algae and the thermal environment. Bacteriol Rev 33:476–504

Costa KC, Navarro JB, Shock EL, Zhang CL, Soukup D, Hedlund BP (2009) Microbiology and geochemistry of great boiling and mud hot springs in the United States Great Basin. Extremophiles 13:447–459

Degryse E, Glansdorff N, Piérard A (1978) A comparative analysis of extreme thermophilic bacteria belonging to the genus *Thermus*. Arch Microbiol 117:189–196

Eder W, Jahnke LL, Schmidt M, Huber R (2001) Microbial diversity of the brine-seawater interface of the Kebrit deep, red sea, studied via 16S rRNA gene sequences and cultivation methods. Appl Environ Microbiol 67:3077–3085

Felsenstein J (1981) Evolutionary trees from DNA sequences: a maximum likelihood approach. J Mol Evol 17:368–376. https://doi.org/10.1007/BF01734359

Felsenstein J (1985) Confidence limits on phylogenies: an approach using the bootstrap. Evolution. https://doi.org/10.1111/j.1558-5646.1985.tb00420.x

Gihring TM, Druschel GK, McCleskey RB, Hamers RJ, Banfield JF (2001) Rapid arsenite oxidation by *Thermus aquaticus* and *Thermus thermophilus*: field and laboratory investigations. Environ Sci Technol 35:3857–3862

Hall TA (2011) Bioedit: an important software for molecular biology. GERF Bull Biosci 2:60–61

Hamamura N, Macur RE, Korf S, Ackerman G, Taylor WP, Kozubal M, Reysenbach AL, Inskeep WP (2009) Linking microbial oxidation of arsenic with detection and phylogenetic analysis of arsenite oxidase genes in diverse geothermal environments. Environ Microbiol 11:421–431. https://doi.org/10.1111/j.1462-2920.2008.01781.x

Hedlund BP, McDonald A, Lam J, Dodsworth JA, Brown J, Hungate B (2011) Potential role of *Thermus thermophilus* and *T. oshimai* in high rates of nitrous oxide (N_2O) production in ~80 °C hot springs in the US Great Basin. Geobiology 9:471–480. https://doi.org/10.1111/j.1472-4669.2011.00295.x

Henne A, Brüggemann H, Raasch C, Wiezer A, Hartsch T, Liesegang H, Johann A, Lienard T, Gohl O, Martinez-Arias R et al (2004) The genome sequence of the extreme thermophile *Thermus thermophilus*. Nat Biotechnol 22:547–553

Johnson DB, Rolfe S, Hallberg KB, Iversen E (2001) Isolation and phylogenetic characterization of acidophilic microorganisms indigenous to acidic drainage waters at an abandoned Norwegian copper mine. Environ Microbiol 3:630–637

Katoh K, Standley D (2013) MAFFT multiple sequence alignment software version 7: improvements in performance and usability. Mol Biol Evol 30:772–780. https://doi.org/10.1093/molbev/mst010

Kieft TL, Fredrickson JK, Onstott TC, Gorby YA, Kostandarithes HM, Bailey TJ, Kennedy DW, Li SW, Plymale AE, Spadoni CM, Gray MS (1999) Dissimilatory reduction of Fe (III) and other electron acceptors by a Thermus isolate. Appl Environ Microbiol 65:1214–1221

Kumar S, Stecher G, Tamura K (2016) MEGA7: molecular evolutionary genetics analysis version 7.0 for bigger datasets. Mol Biol Evol 33:1870–1874. https://doi.org/10.1093/molbev/msw054

McMurdie P, Holmes S (2013) phyloseq: an R package for reproducible interactive analysis and graphic of microbiome census data. PLoS ONE 8:1217. https://doi.org/10.1371/journal.pone.0061217

Mefferd CC, Zhou E-M, Yu T-T, Ming H, Murugapiran SK, Huntemann M, Clum A, Pillay M, Palaniappan K, Varghese N, Mikhailova N, Stamatis D, Reddy TBK, Ngan CY, Daum C, Duffy K, Shapiro N, Markowitz V, Ivanova N, Kyrpides N, Williams AJ, Woyke T, Li W-J, Hedlund BP (2016) High-quality draft genomes from *Thermus caliditerrae* YIM 77777 and *T. tengchongensis* YIM 77401, isolates from Tengchong. China Genome Announc 4:e00312–e316. https://doi.org/10.1128/genomeA.00312-16

Miller-Coleman RL, Dodsworth JA, Ross CA, Shock EL, Williams AJ, Hartnett HE, McDonald AI, Havig JR, Hedlund BP (2012)

Korarchaeota diversity, biogeography, and abundance in Yellowstone and Great Basin hot springs and ecological niche modeling based on machine learning. PLoS ONE 7:e35964. https://doi.org/10.1371/journal.pone.0035964

Ming H, Yin YR, Li S, Nie GX, Yu TT, Zhou EM, Liu L, Dong L, Li WJ (2014) *Thermus caliditerrae* sp. nov., a novel thermophilic species isolated from a geothermal area. Int J Syst Evol Microbiol 64:650–656. https://doi.org/10.1099/ijs.0.056838-0

Möller C, van Heerden E (2006) Isolation of a soluble and membrane-associated Fe(III) reductase from the thermophile, *Thermus scotoductus* (SA-01). FEMS Microbiol Lett 265:237–243

Moser DP, Nealson KH (1996) Growth of the facultative anaerobe *Shewanella putrefaciens* by elemental sulfur reduction. Appl Environ Microbiol 62:2100–2105

Murphy CN, Dodsworth JA, Babbitt AB, Hedlund BP (2013) Community microrespirometry and molecular analyses reveal a diverse energy economy in Great Boiling Spring and Sandy's Spring West in the US. Great Basin Appl Environ Microbiol 79:3306–3310. https://doi.org/10.1128/AEM.00139-13

Murugapiran SK, Huntemann M, Wei CL, Han J, Detter JC, Han CS, Erkkila TH, Teshima H, Chen A, Kyrpides N, Mavrommatis K, Markowitz V, Szeto E, Ivanova N, Pagani I, Lam J, McDonald AI, Dodsworth JA, Pati A, Goodwin L, Peters L, Pitluck S, Woyke T, Hedlund BP (2013) *Thermus oshimai* JL-2 and *T. thermophilus* JL-18 genome analysis illuminates pathways for carbon, nitrogen, and sulfur cycling. Stand Genom Sci 7:449–468. https://doi.org/10.4056/sigs.3667269

Pan C, Banfield JF (2014) Quantitative metaproteomics: functional insights into microbial communities. Methods Mol Biol 1096:231–240. https://doi.org/10.1007/978-1-62703-712-9_18

Pantazaki A, Pritsa A, Kyriakidis D (2002) Biotechnologically relevant enzymes from *Thermus thermophilus*. Appl Microbiol Biotechnol 58:1–12. https://doi.org/10.1007/s00253-001-0843-1

Park CY, Klammer AA, Käll L, MacCoss MJ, Noble WS (2008) Rapid and accurate peptide identification from tandem mass spectra. J Proteome Res 7:3022–3027. https://doi.org/10.1021/pr800127y

Saitou N, Nei M (1987) The neighbor-joining method: a new method for reconstructing phylogenetic trees. Mol Biol Evol 4:406–425. https://doi.org/10.1093/oxfordjournals.molbev.a040454

Sazanov LA, Hinchliffe P (2006) Structure of the hydrophilic domain of respiratory complex I from *Thermus thermophilus*. Science 311:1430–1436

Schloss PD, Westcott SL, Ryabin T, Hall JR, Hartmann M, Hollister EB, Lesniewski RA, Oakley BB, Parks DH, Robinson CJ, Sahl JW, Stres B, Thallinger GG, Van Horn DJ, Weber CF (2009) Introducing mothur: open-source, platform-independent, community-supported software for describing and comparing microbial communities. Appl Environ Microbiol 75:7537–7541. https://doi.org/10.1128/AEM.01541-09

Skirnisdottir S, Hreggvidsson GO, Holst O, Kristjansson JK (2001) Isolation and characterization of a mixotrophic sulfur-oxidizing *Thermus scotoductus*. Extremophiles 5:45–51. https://doi.org/10.1007/s007920000172

Vick T, Dodsworth JA, Costa K, Shock E, Hedlund BP (2010) Microbiology and geochemistry of Little Hot Creek, a hot spring environment in the Long Valley Caldera. Geobiology 8:140–154. https://doi.org/10.1111/j.1472-4669.2009.00228.x

Vieille C, Zeikus GJ (2001) Hyperthermophilic enzymes: sources, uses, and molecular mechanisms for thermostability. Microbiol Mol Biol Rev 65:1–43

Whitaker RJ, Grogan DW, Taylor JW (2003) Geographic barriers isolate endemic populations of hyperthermophilic archaea. Science 301:976–978

Wickham H (2009) ggplot2: elegant graphics for data analysis. Springer, New York

Yu TT, Yao JC, Ming H, Yin YR, Zhou EM, Liu MJ, Tang SK, Li WJ (2013) *Thermus tengchongensis* sp. nov., isolated from a geothermally heated soil sample in Tengchong Yunnan, south-west China. Antonie Van Leeuwenhoek 103:513–518. https://doi.org/10.1007/s10482-012-9833-9

Yusupov MM, Yusupova GZ, Baucom A, Lieberman K, Earnest TN, Cate J, Noller HF (2001) Crystal structure of the ribosome at 5.5 Å resolution. Science 292:883–896

Zhou EM, Xian WD, Mefferd CC, Thomas SC, Adegboruwa AL, Williams N, Murugapiran SK, Dodsworth JA, Ganji R, Li MM, Ding YP, Liu L, Woyke T, Li WJ, Hedlund BP (2018) *Thermus sediminis* sp. nov., a thiosulfate-oxidizing and arsenate-reducing organism isolated from Little Hot Creek in the Long Valley Caldera. California Extremophiles 22:983–991. https://doi.org/10.1007/s00792-018-1055-2